NREL
NATIONAL RENEWABLE ENERGY LABORATORY

Estimating the Wind Resource in Uttarakhand: Comparison of Dynamic Downscaling with Doppler Lidar Wind Measurements

J.K. Lundquist and A. Purkayastha
National Renewable Energy Laboratory

C. St. Martin
University of Colorado, Boulder

R. Newsom
Pacific Northwest National Laboratory

NREL is a national laboratory of the U.S. Department of Energy
Office of Energy Efficiency & Renewable Energy
Operated by the Alliance for Sustainable Energy, LLC

This report is available at no cost from the National Renewable Energy Laboratory (NREL) at www.nrel.gov/publications.

Technical Report
NREL/TP-5000-61103
March 2014

Contract No. DE-AC36-08GO28308

NREL
NATIONAL RENEWABLE ENERGY LABORATORY

Estimating the Wind Resource in Uttarakhand: Comparison of Dynamic Downscaling with Doppler Lidar Wind Measurements

J.K. Lundquist and A. Purkayastha
National Renewable Energy Laboratory

C. St. Martin
University of Colorado, Boulder

R. Newsom
Pacific Northwest National Laboratory

Prepared under Task No. WFK6.1002

National Renewable Energy Laboratory
15013 Denver West Parkway
Golden, CO 80401
303-275-3000 • www.nrel.gov

Technical Report
NREL/TP-5000-61103
March 2014

Contract No. DE-AC36-08GO28308

This report is available at no cost from the National Renewable Energy Laboratory (NREL) at www.nrel.gov/publications.

Available electronically at http://www.osti.gov/scitech

Available for a processing fee to U.S. Department of Energy and its contractors, in paper, from:

U.S. Department of Energy
Office of Scientific and Technical Information
P.O. Box 62
Oak Ridge, TN 37831-0062
phone: 865.576.8401
fax: 865.576.5728
email: mailto:reports@adonis.osti.gov

Available for sale to the public, in paper, from:

U.S. Department of Commerce
National Technical Information Service
5285 Port Royal Road
Springfield, VA 22161
phone: 800.553.6847
fax: 703.605.6900
email: orders@ntis.fedworld.gov
online ordering: http://www.ntis.gov/help/ordermethods.aspx

Cover Photos: (left to right) photo by Pat Corkery, NREL 16416, photo from SunEdison, NREL 17423, photo by Pat Corkery, NREL 16560, photo by Dennis Schroeder, NREL 17613, photo by Dean Armstrong, NREL 17436, photo by Pat Corkery, NREL 17721.

Printed on paper containing at least 50% wastepaper, including 10% post consumer waste.

Nomenclature or List of Acronyms

ARM	Atmospheric Radiation Measurement
BAT	Define acronyms
DOE	U.S. Department of Energy
GVAX	Ganges Valley Aerosol Experiment
HPC	High performance computing
MAE	Mean absolute error
MDE	Median absolute error
MF	Mobile facility
NREL	National Renewable Energy Laboratory
RSME	Root mean square error
WRF	Weather Research and Forecasting

Executive Summary

Standard methods of wind resource assessment often rely on extrapolation of winds and use coarse computational grids to address the effects of complex terrain on atmospheric flow. Further, even if measurements are available in complex terrain, those measurements may not be representative of the flow nearby if the terrain differs significantly. Previous estimates of the wind resources in Uttarakhand, India, indicated that there were minimal wind resources in this region. To explore whether or not complex terrain in the region in fact provides localized areas of increased wind resource, we employed a dynamic downscaling method using the Weather Research and Forecasting model to provide detailed estimates of wind speeds at approximately 1-km horizontal resolution in the finest nested simulation. The only measurements available in the region for verification are from a 9-month Doppler lidar deployment. As this region experiences three distinct seasons, one 7–10 day period from each season was selected from the period during which Doppler lidar data were available. Hourly estimates of Doppler lidar wind speed and wind direction were calculated and compared with simulated winds. The simulations generally underestimated the observed wind speed: lidar observations indicate average wind speeds of at least 6.3 m/s in each of the periods simulated. Although localized pockets of higher wind resource were evident at altitudes of 80–100 m above the surface, the general resource in Uttarakhand could be characterized as minimal from the simulations, with average wind speeds equal to or below the typical turbine cut-in speed of ~ 3 m/s^{-1} or less at 80–100 m above the surface. However, the results of these simulations do not constitute a definitive wind resource assessment. More extensive observations at other sites within this region and at wind-energy-relevant altitudes are required to validate the simulations' estimates of the wind resource in Uttarakhand. This region could provide a valuable wind resource in proximity to large population centers, and the few existing observations suggest some wind resource was not captured with the simulations. Future wind resource estimation efforts should include deployment of observational platforms (such as lidar or meteorological towers) in several of the lower-altitude valleys of Uttarakhand over the course of a year. These observations could then be compared with a larger set of simulations similar to those executed for this study to assess the ability of Uttarakhand to provide a valuable resource of renewably-generated electricity.

Table of Contents

List of Figures

1 Introduction

Complex terrain can induce strong wind flows that can produce significant wind resources (Whiteman 2000). If peaks and valleys are not represented in simulations, however, the effects of terrain on flows cannot emerge in the simulations. Wind resource assessment in complex terrain is particularly challenging because of the nature of topographically driven flows (Brower, 2012). The speed, direction, and daily cycle of these flows tend to be poorly represented in typical wind resource assessment approaches, therefore a refined modeling approach that captures these complex flows may be appropriate. Such a modeling approach consists of mesoscale numerical weather prediction simulations for a region of interest for a limited time period. These simulations are computationally intensive and require validation with field observations.

The Uttarahkand region of northeastern India was chosen as a candidate for exploration of the advantages of using high-resolution mesoscale modeling for wind resource assessment because of Uttarakhand's complex terrain and proximity to the population center of New Delhi: transmission of renewably generated electricity to this large population center would be desirable. Although India as a nation had approximately 20 GW of installed wind capacity as of Oct. 31, 2013 (Ministry of New and Renewable Energy, 2013), based on previous wind resource assessments (Centre for Wind Technologies (CWET), 2013), Uttarahkand appeared to have minimal wind development potential. As summarized by Hossain et al. (2011), wind energy resources in India have historically been underestimated. Further, northeastern Uttarakhand includes the very complex terrain of the Himalayas, which made this region a robust challenge for mesoscale modeling in complex terrain. A recent analysis of detailed meteorological observations in a mountain pass in Switzerland (Clifton et al., 2013) suggests that mountainous regions may in fact be suitable for wind energy development due to the channeling of flow. Finally, a brief period of atmospheric observations in Uttarakhand was available from the Ganges Valley Aerosol Experiment (GVAX) sponsored by the U.S. Department of Energy's (DOE's) Atmospheric Radiation Measurement Program and conducted under an existing Science and Technology Cooperation Agreement between the governments of the United States of America and the Republic of India (see http://www.arm.gov/campaigns/amf2011gvax for more information). These refined observations, which were collected from June 2011 to March 2012, included detailed wind profiles in the lower atmospheric boundary layer from a Doppler lidar dataset (data provided by the U.S. Department of Energy's Pacific Northwest National Laboratory).

This report explores the ability of dynamically downscaled simulations to assess wind resources in Uttarakhand and compares these simulations to the only boundary-layer wind profile data known for the region, the Doppler lidar dataset available from one location in the region. The simulations and the lidar observations are described in detail in Section 2. Section 3 explores simulation results, including the impact of horizontal resolution on the simulations and the vertical variability of the wind resource. Although meteorological data for only one location were available for model validation, agreement between the simulations and the observations was also assessed, and a comparison between these simulations and previous wind resources assessments in the region is presented. Finally, this report summarizes the diurnal variability in the wind resource based on observations.

2 Data and Methods

2.1 Mesoscale Simulations

Numerous modeling studies have indicated the importance of high-resolution topographic databases for accurate simulations of winds near the surface and at wind turbine altitudes. Regional models, with smaller domains and finer resolutions than global models, can better resolve small-scale features (such as terrain variations) that depend on the surface boundary (Castro et al., 2005). Therefore, global-scale simulations are typically refined by using a limited-area model at finer resolution for the domain of interest. Initial conditions and boundary conditions are provided by a global model, while a regional climate model adds detail and refinement in response to regional scale forcing (e.g., topography, coastlines, and land use/land cover data) as the regional model interacts with the larger-scale atmospheric circulations. The purpose of downscaling is to obtain high-resolution detail as accurately as possible for the region of interest.

Numerous studies demonstrate the utility of dynamic downscaling. An investigation of more than a decade of high-wind events in the Sierra Mountains of California (Hughes et al., 2012) demonstrates that 6-km resolution dynamically downscaled simulations are required to achieve good agreement with radar wind profiler observations as compared to coarser-scale reanalysis data. Simulations of the complex terrain around Greenland (DuVivier and Cassano, 2013) using the Weather Research and Forecasting (WRF) model at 10-km horizontal resolution were superior to the simulations at coarser resolutions. An investigation of precipitation forecasting in the Himalayan region (Dimri et al., 2014) also emphasizes the importance of high-resolution simulations.

For this exploration of the utility of dynamic downscaling of wind resources in Uttarakhand, simulations of the atmospheric flow were performed with the WRF numerical weather prediction model (Skamarock et al. 2008). Initial and boundary conditions for these simulations came from the Global Forecasting System Extended (global) one-half degree archive (Unidata, 2013), which provided updates every six hours. Forty vertical levels were used, with 13 levels in the lowest 300 m of the atmosphere to ensure high resolution of the boundary layer in the complex terrain. The four domains were one-way nested by a factor of three, with the outermost domain at 30-km resolution, the second at 10-km resolution, the third at 3.33-km resolution, and the fourth at 1.1-km resolution. Each domain consisted of 100 cells by 100 cells, as shown in Figure 1 and Figure 2, and the Doppler lidar observation station is located in the center of Domain 4. The time step for the outer domain was 10 seconds and was reduced by a factor of three with each consecutive nest. Cloud microphysics were parameterized with the Morrison double-moment scheme. Cumulus clouds were parameterized with the Kain-Fritsch scheme on the outer three domains. Longwave radiation was parameterized with the Rapid Radiative Transfer (RRTM) model, and shortwave radiation was parameterized with the Dudhia scheme. The surface layer and the planetary boundary layer were parameterized with the Mellor Yamada Nakanishi Niino (MYNN2) models (Nakanishi and Niino, 2006). Computational resource limitations required execution of only a single deterministic simulation for each of the time periods examined here, although an ensemble of simulations exploring the influence of model physics choices would provide insight into variability (Mahoney et al., 2012). Alternatively, reliable uncertainty quantification could be provided with hybrid statistical-dynamic downscaling techniques such as

the analog ensemble presented by Delle Monache et al. (2013), which would require a single deterministic simulation to generate an analog ensemble if more observations were available for inclusion.

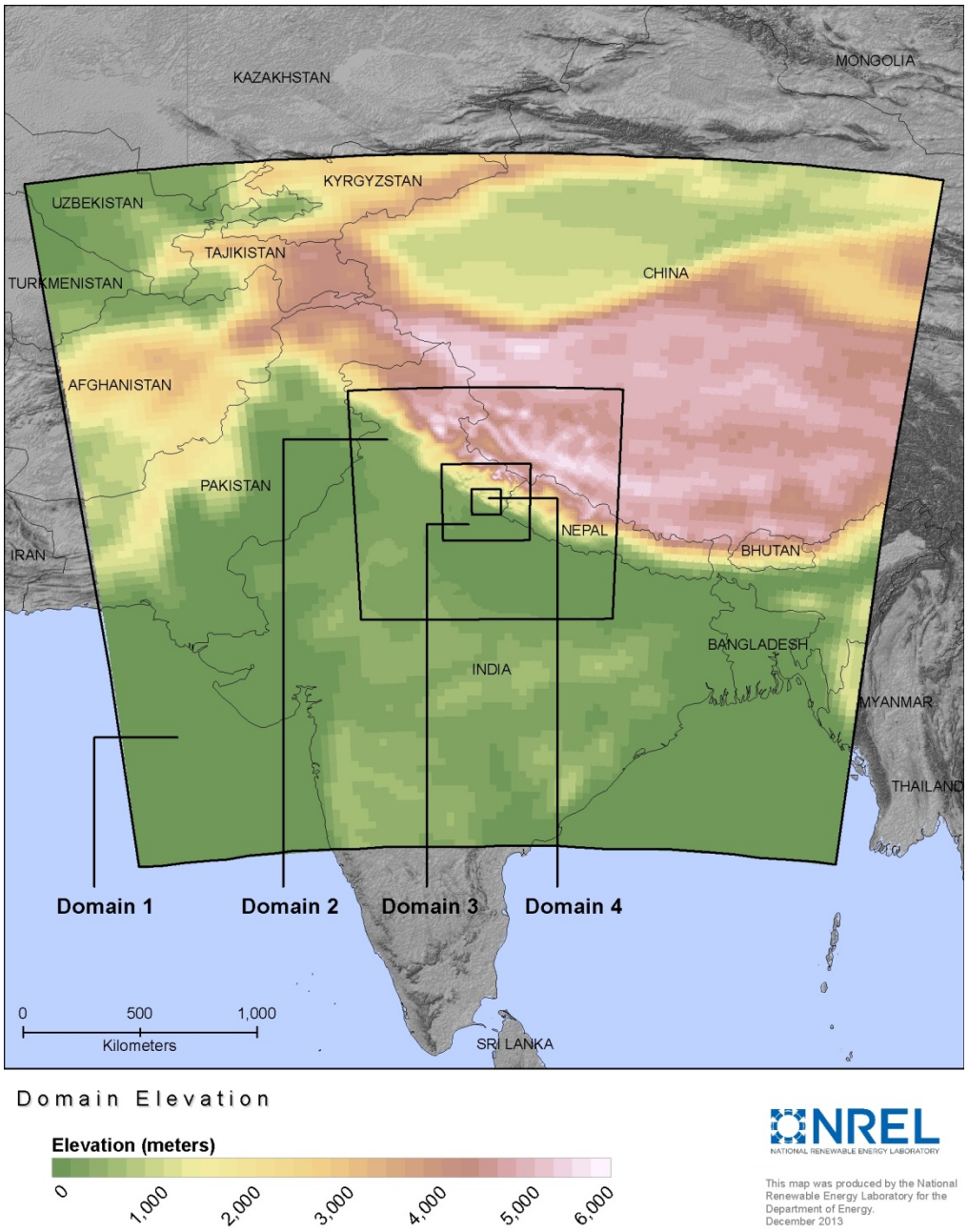

Figure 1: Map of WRF simulation domains. The spatial resolution of Domains 1, 2, 3, and 4 is 30-, 10-, 3.3-, and 1.1-km, respectively. The observation station is located in the center of Domain 4.

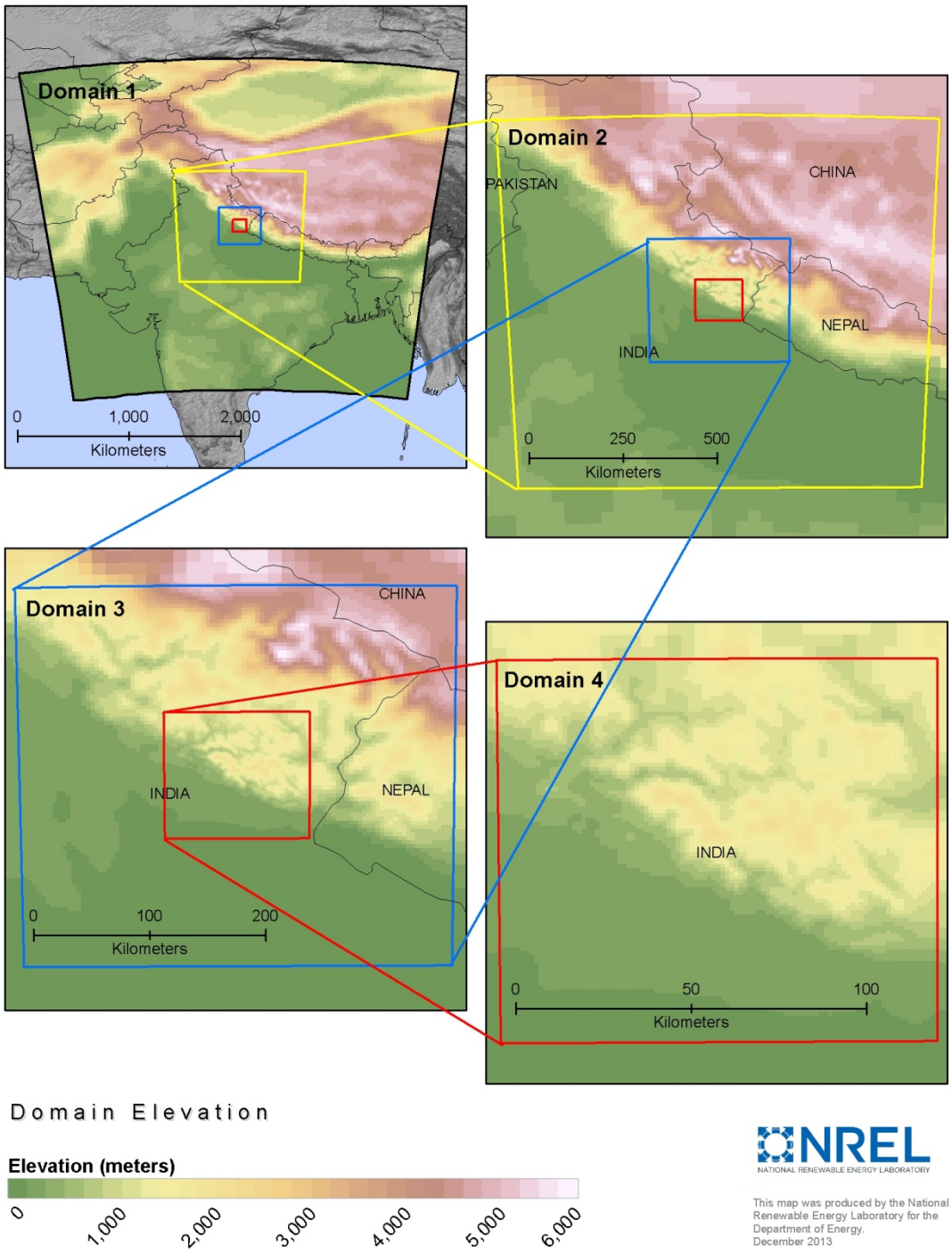

Figure 2: Detailed map of WRF simulation domains. The observation station is located in the center of Domain 4.

Although simulations for an entire year or several years (Brower et al., 2012) or the selection of representative days over several years (Rife et al., 2013) would be preferable for a wind resource assessment, computational and data comparison constraints required a selection of representative seasons from one year. Uttarakhand has three primary seasons: summer (March to June), winter (October to February), and monsoon (July to September)[1]. The availability of lidar data for comparison also constrained the choice of observational periods, as data was only available from June 2011 to March 2012. The simulations for this analysis were performed for eight days in August (monsoon), nine days in October and November (winter), and seven days in March (summer). For all three seasons, the complete simulation runs required approximately 2,470 node hours.

2.2 Lidar Observations

Conventional wind resource assessment campaigns rely on observations collected throughout a region, rather than the limited set of observations from one location available here. The U.S. Department of Energy's Atmospheric Radiation Measurement (ARM) Program's mobile facility (MF) participated in the Ganges Valley Aerosol Experiment (GVAX) that explored the effects of atmospheric aerosols in the Ganges Valley of Uttarahand on cloud formation and monsoon activity over the Indian Ocean (http://www.arm.gov/campaigns/amf2011gvax). Although most of the ARM instrument deployments for GVAX focused on measurements of aerosols and their effects on atmospheric radiation, the deployment of a Doppler Lidar (DL) provided detailed measurements of winds at one location, the ARIES Observatory in Nainital, Uttarakhand, from June 2011 to March 2012. (ARIES is the Aryabhatta Research Institute of Observational-SciencES, known as ARIES since 2004.) No other measurements of wind at altitudes relevant for wind energy were identified.

The ARM MF Doppler lidar (DL) is described in Newsom (2012). As an active remote sensing instrument, it provides range- and time-resolved measurements of radial velocity; multiple vertical scans can be aggregated together to provide profiles of horizontal winds. The DL operates in the near-infrared (1.5 microns) and is sensitive to backscatter from micron-sized aerosols. Aerosols are ubiquitous in the low troposphere and are ideal tracers of atmospheric winds. The DL is capable of measuring wind velocities under clear-sky conditions with very good precision (typically ~10 cm/sec). Profiles of the mean winds are derived from hourly plan-position-indicator (PPI) scan data using a modified velocity-azimuth display algorithm (Banta et al. 2002, Browning et al. 1968).

The lidar data returns for hourly averages of wind speed at altitudes between 40 m and 500 m were generally of very good quality(Figure 3) except for the August time period, when heavy precipitation influenced the ability of the lidar to collect wind speed measurements. Wind speeds at approximately 80 m above the surface exhibited considerable variability (Figure 4-Figure 6) with overall maximum wind speeds ~15–18 m/s. Doppler lidar measurements indicated the average wind speed for the weeks selected in each season at approximately 80 m above the

[1] Traditionally, Indians recognize six seasons or *Ritu*, each about two months long. The six seasons include spring, summer, monsoon, autumn, winter, and prevernal. As Uttarakhand is located in the Himalayan foothills, its seasons vary from those of other parts of India.

surface is from 6.3 m/s (November and August) to 6.6 m/s (March). As expected, mean wind speeds are higher at approximately 100 m above the surface: November and August have average wind speeds of 6.6 m/s while March shows an average wind speed of 6.7 m/s. The number of data points available for consideration (less than 200) are not sufficient for estimating the underlying distribution (such as a Weibull distribution).

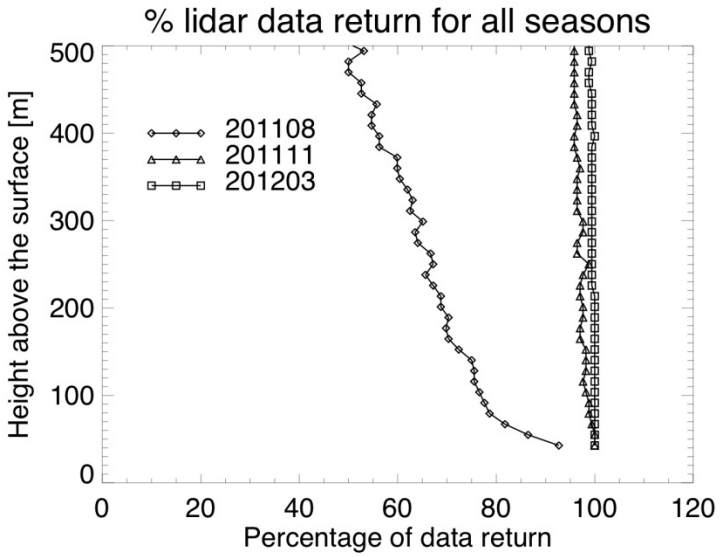

Figure 3: Percentage of Doppler lidar data return from each of the three seasons

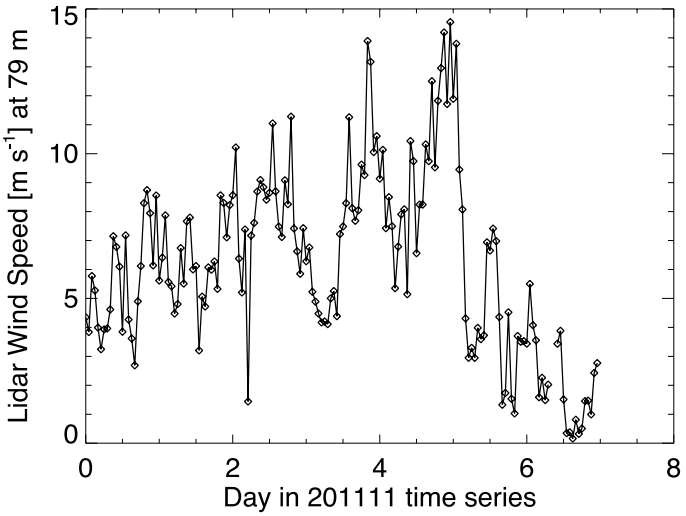

Figure 4: Time series of wind speeds at ~ 80-m elevation measured by the Doppler lidar during the November set of simulations.

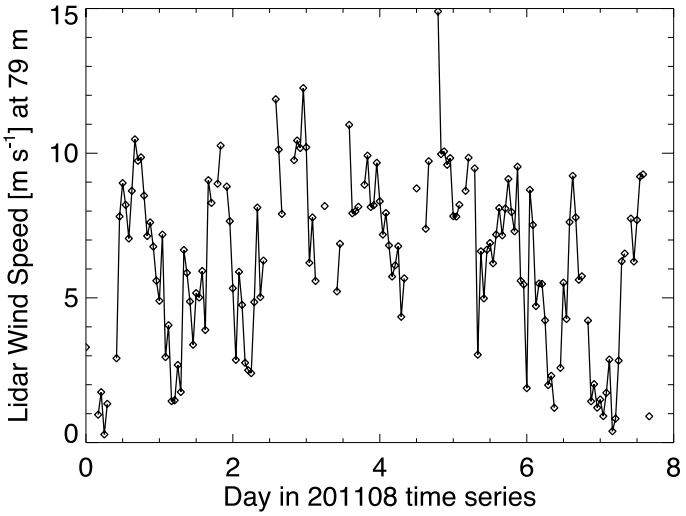

Figure 5: Time series of wind speeds at ~ 80-m elevation measured by the Doppler lidar during the August set of simulations.

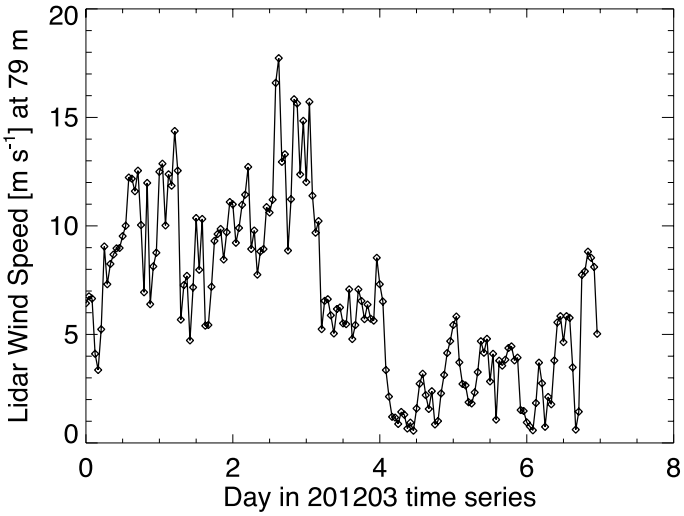

Figure 6: Time series of wind speeds at ~ 80-m elevation measured by the Doppler lidar during the March set of simulations

3 Results

3.1 Impact of Horizontal Resolution on Wind Resource Estimates

Complex terrain can induce strong wind flows that can produce significant wind resources (Whiteman 2000). If peaks and valleys are not represented in simulations, however, the effects of terrain on flows cannot emerge in the simulations. Increased horizontal resolution provided by the downscaled numerical weather prediction model can theoretically identify areas of wind resource that would have been overlooked with coarser-scale simulations. A comparison of the coarse simulations for November (Figure 7-Figure 9) to the finest simulations for that month (Figure 10) revealed that the strong averaged wind resource of the finest domain in the valleys in the northwest are overlooked by the coarse simulations which cannot resolve those valleys. The finest-scale simulations suggest strong average winds in isolated valleys in northwestern Uttarakhand (5 km south of Patti Gujru). It is likely that even finer-scale simulations could identify other regions of significant resource.

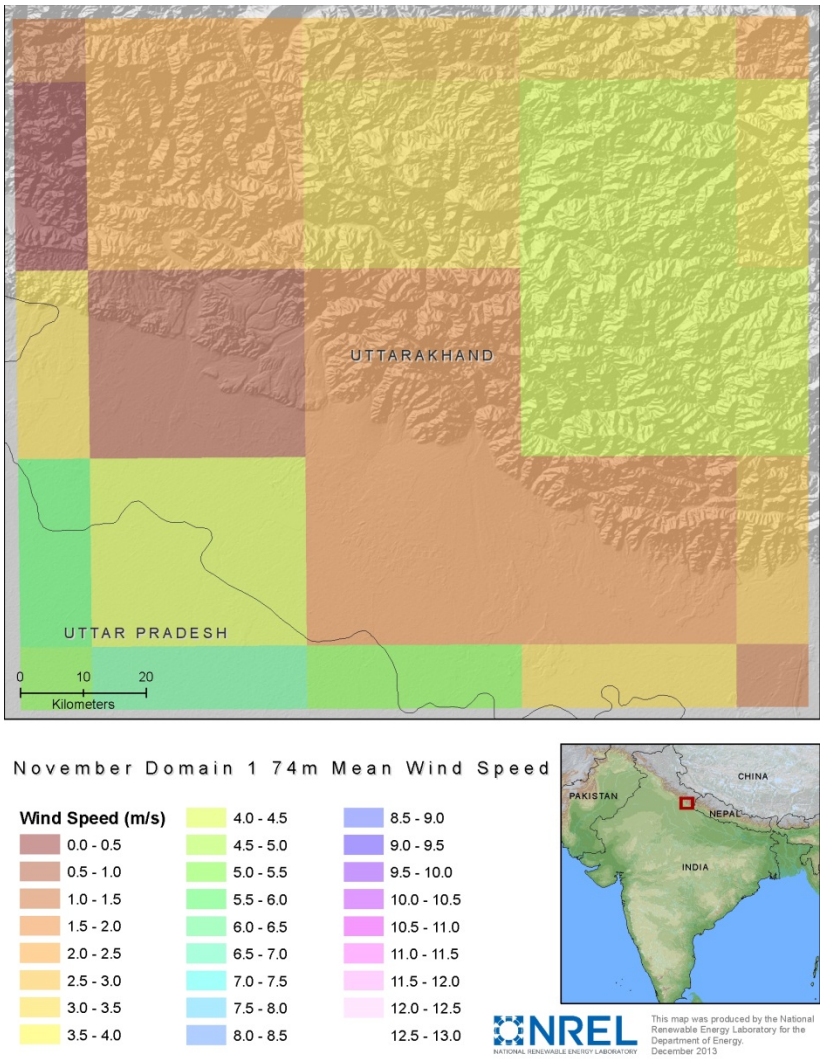

Figure 7: Average wind speed at approximately 80-m above the surface from 30-km resolution simulations of 1-7 Nov 2011

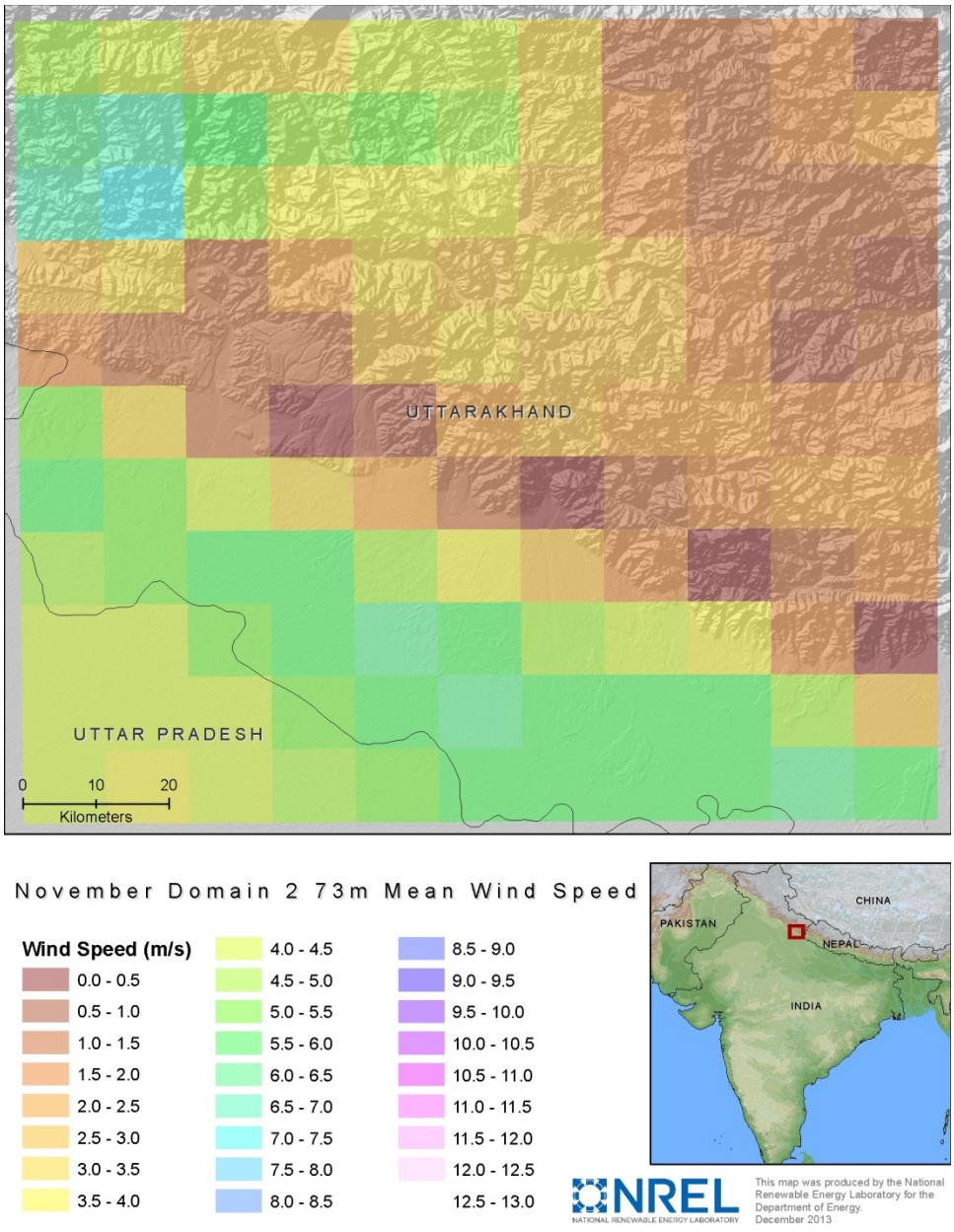

Figure 8: Average wind speed at approximately 80-m above the surface from 10-km resolution simulations of 1-7 Nov 2011

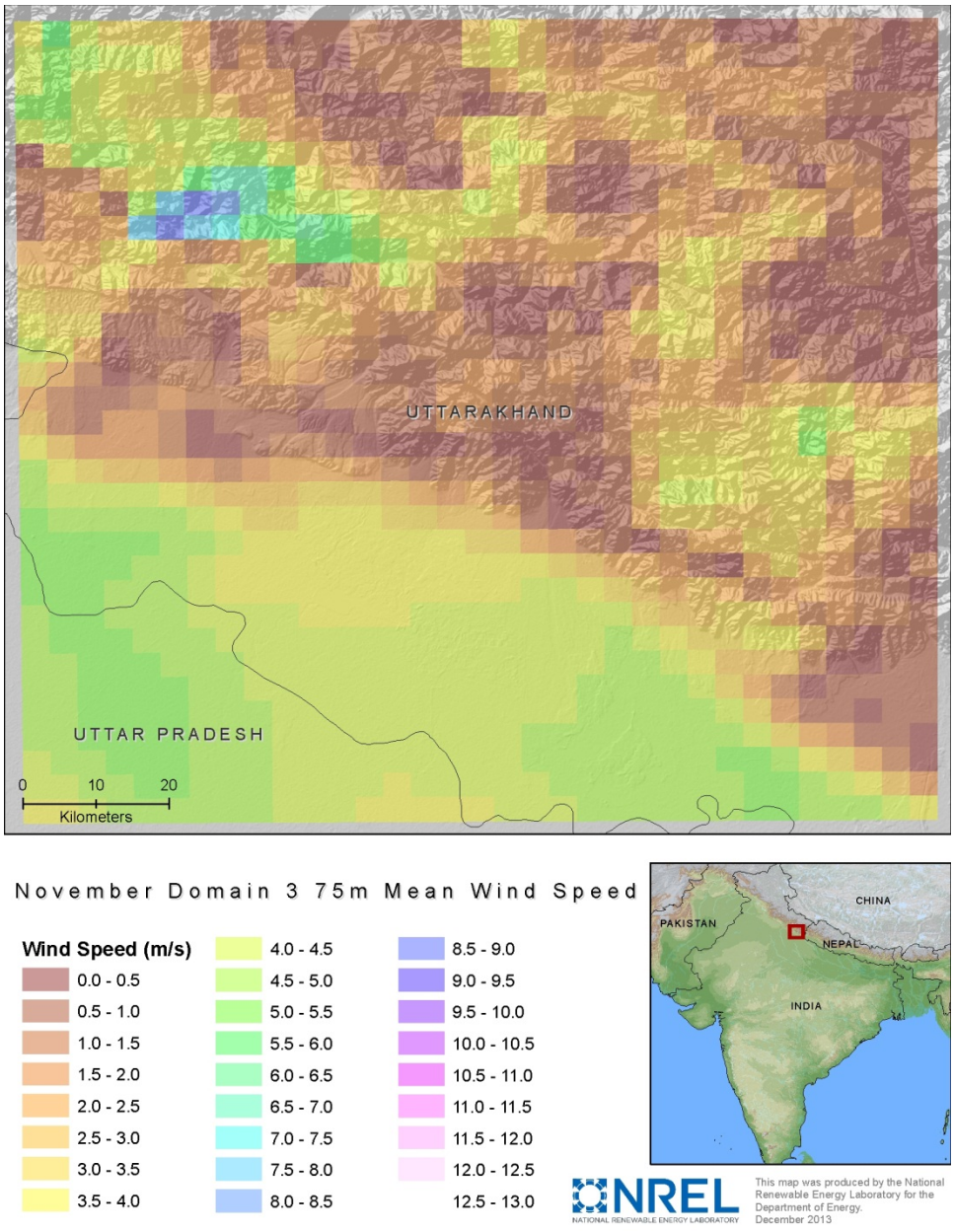

Figure 9: Average wind speed at approximately 80-m above the surface from 3.33-km resolution simulations of 1-7 Nov 2011

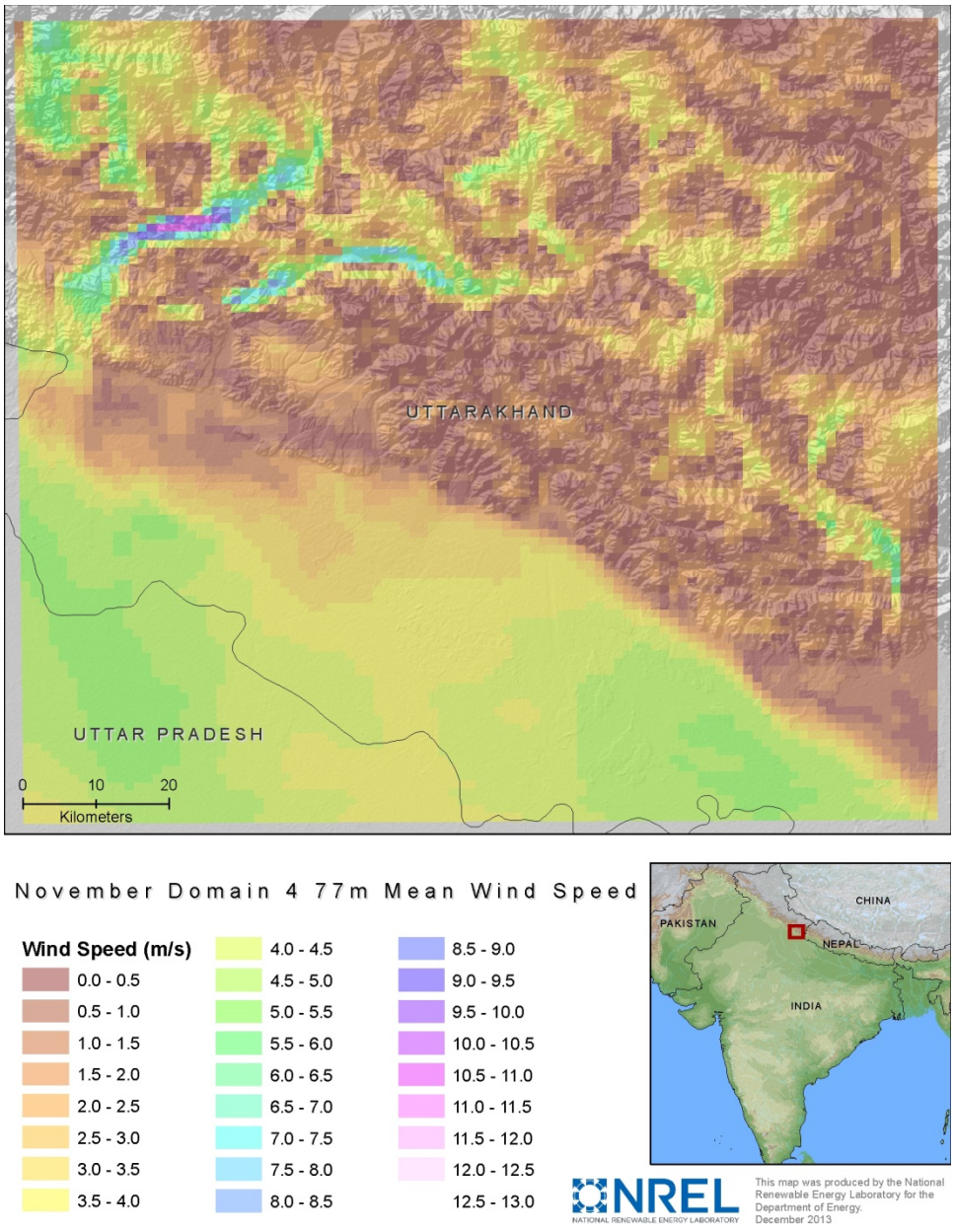

Figure 10: Average wind speed at approximately 80-m above the surface from 1.1-km resolution simulations of 1-7 Nov 2011

Simulations in August (Figure 11 - Figure 14) and March (Figure 15 - Figure 18) show similar patterns, although the overall wind speeds are very low, typically below the turbine cut-in speed of 3.0 m/s.

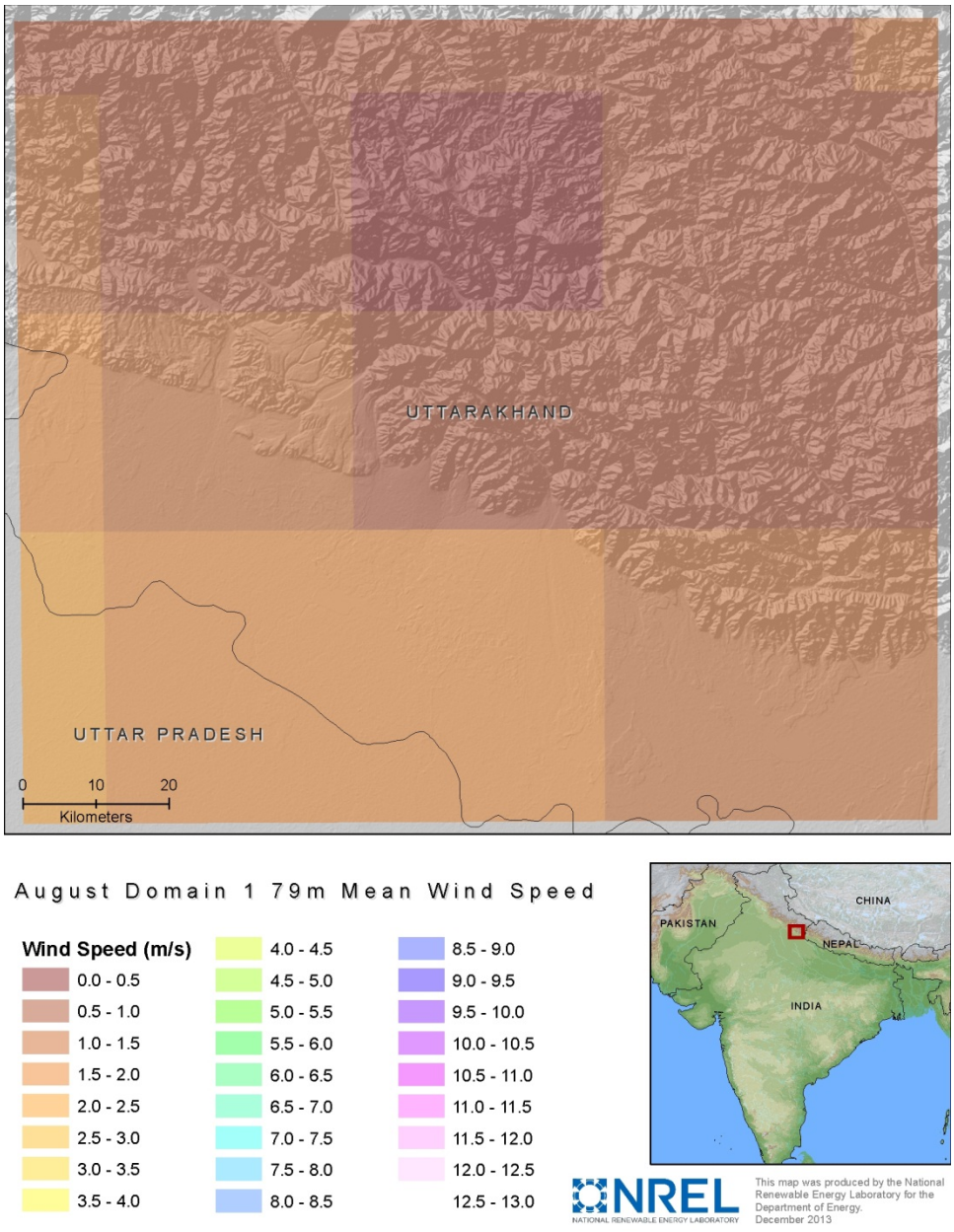

Figure 11: Average wind speed at approximately 80-m above the surface from 30-km resolution simulations of 8-15 Aug 2011

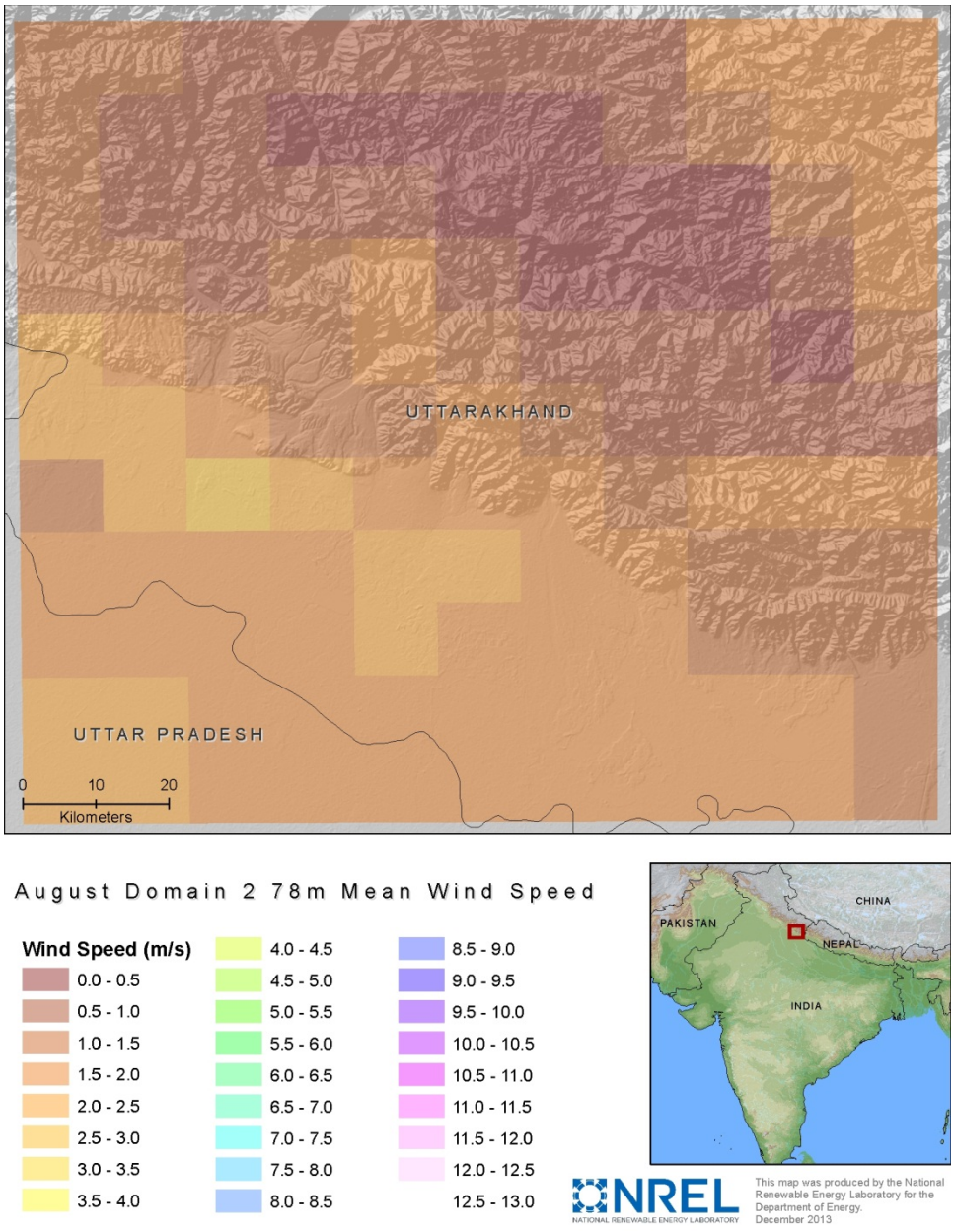

Figure 12: Average wind speed at approximately 80-m above the surface from 10-km resolution simulations of 8-15 Aug 2011

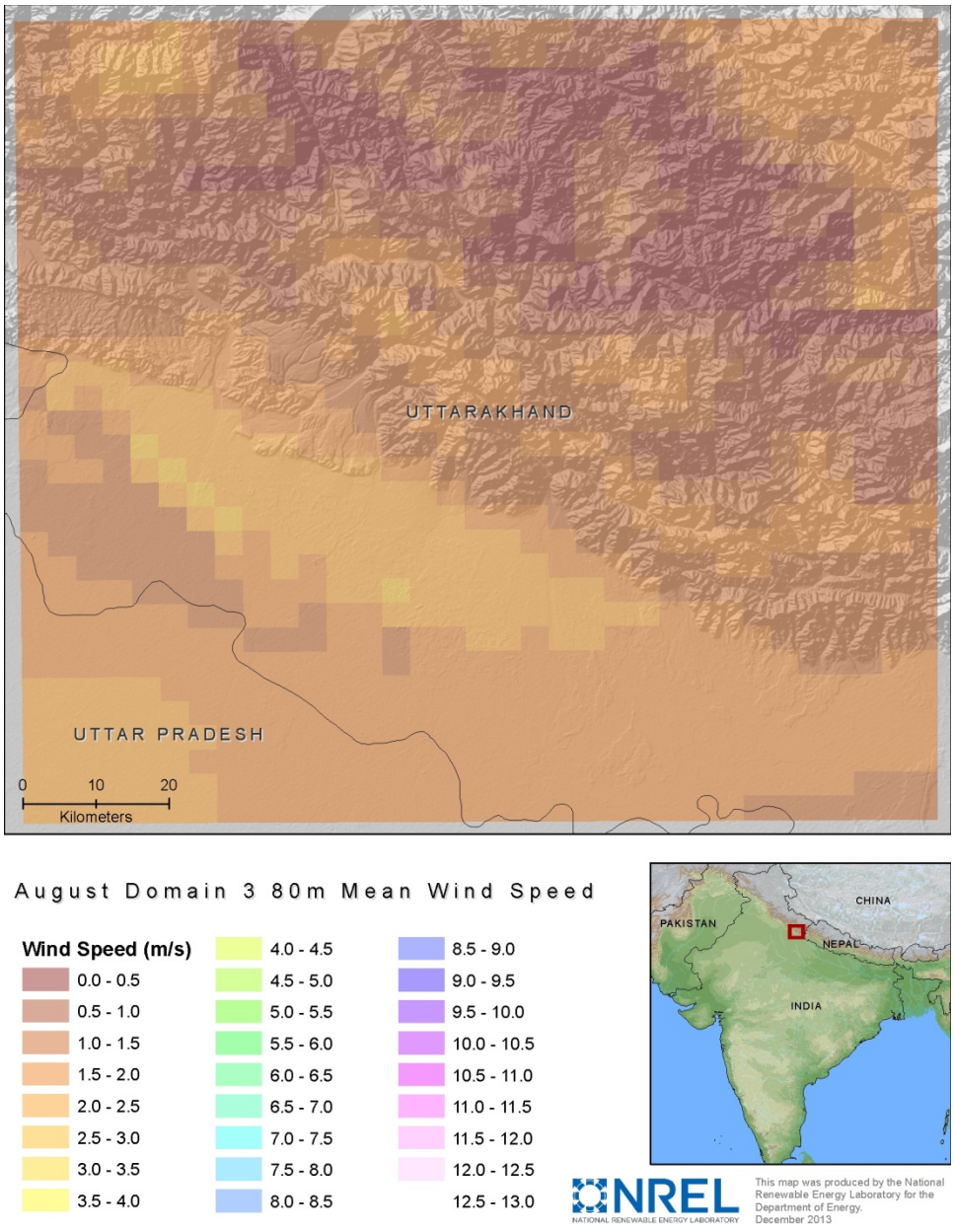

Figure 13: Average wind speed at approximately 80-m above the surface from 3.3-km resolution simulations of 8-15 Aug 2011

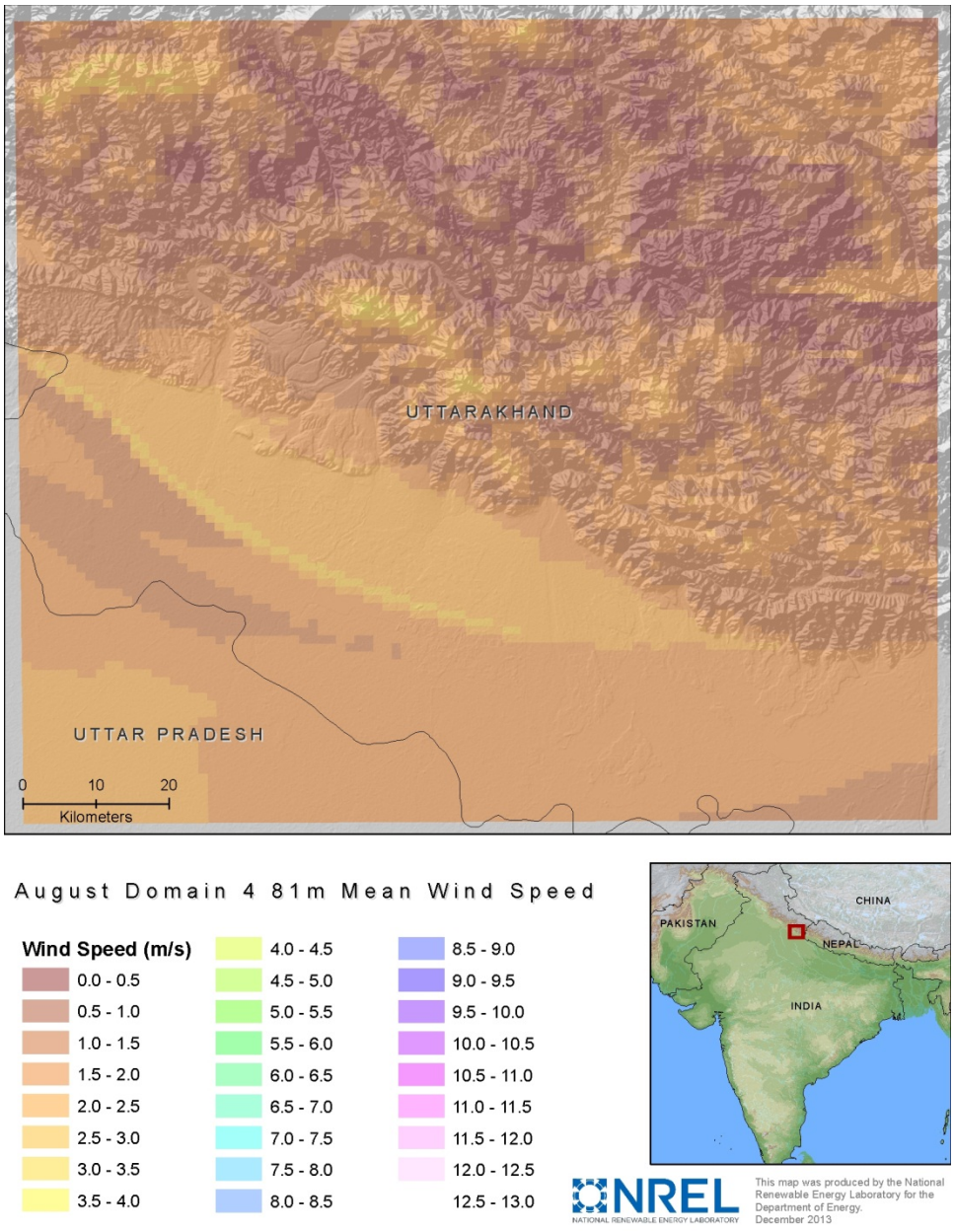

Figure 14: Average wind speed at approximately 80-m above the surface from 1.1-km resolution simulations of 8-15 Aug 2011

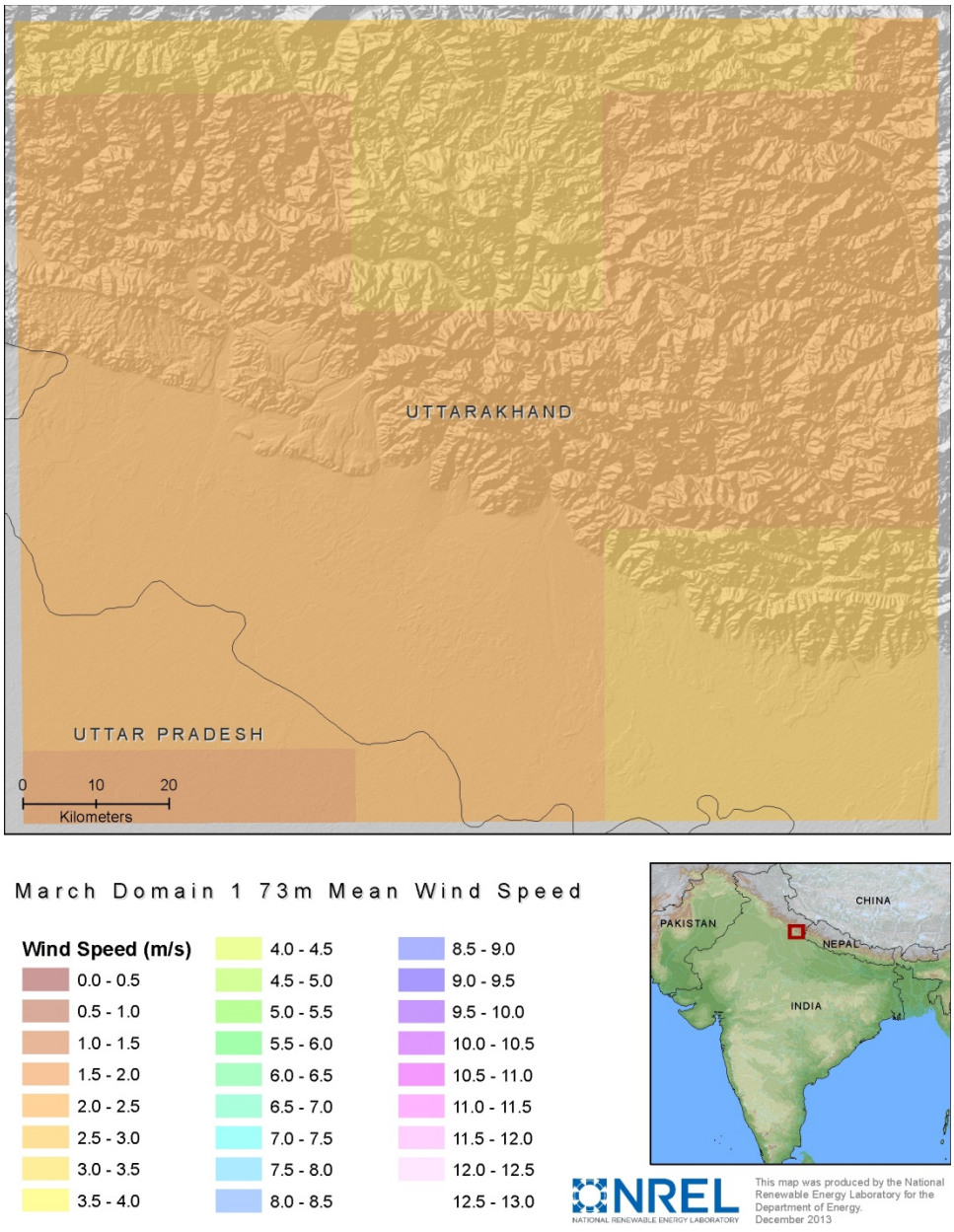

Figure 15: Average wind speed at approximately 80-m above the surface from 30-km resolution simulations of 1-8 Mar 2012

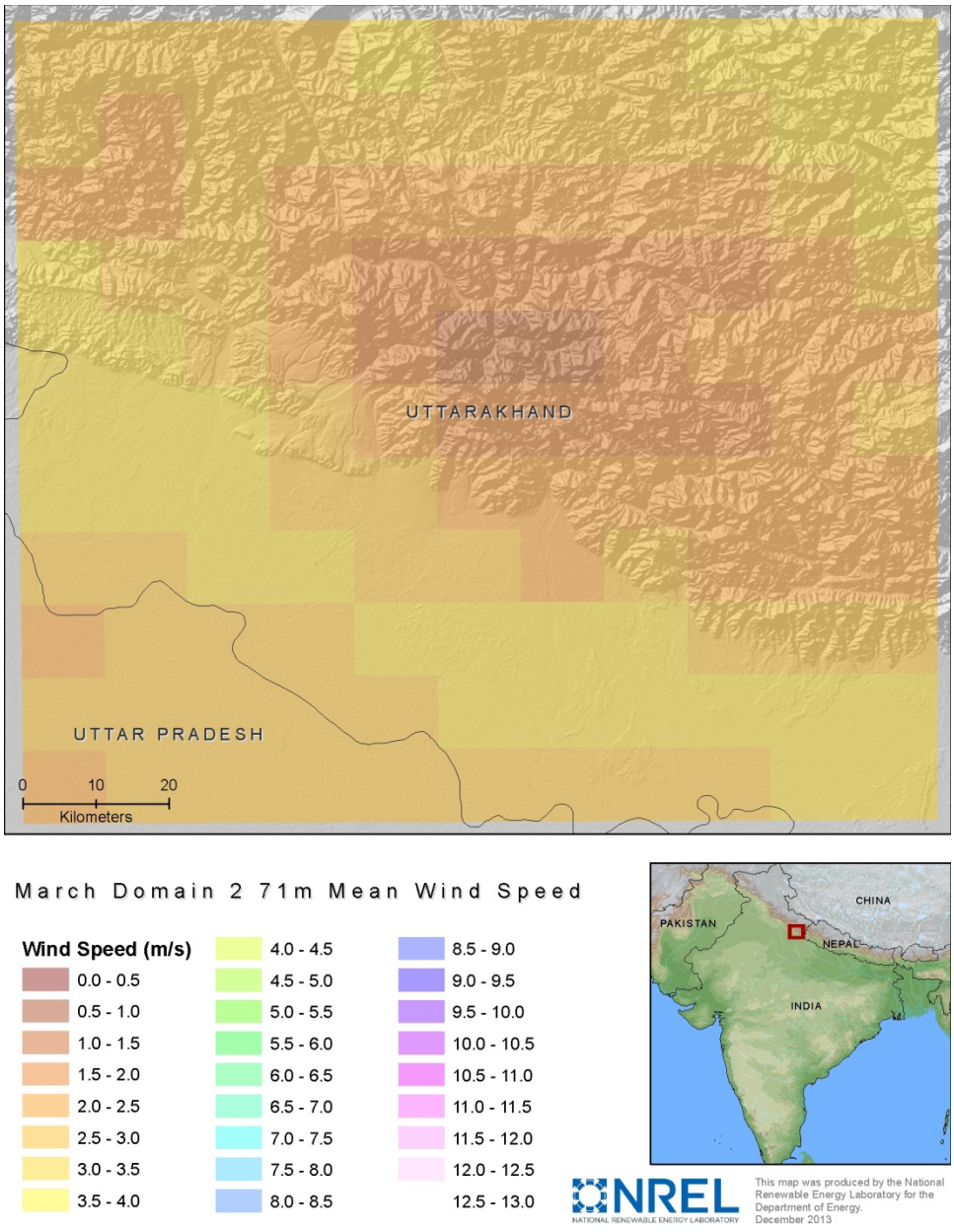

Figure 16: Average wind speed at approximately 80-m above the surface from 10-km resolution simulations of 1-8 Mar 2012

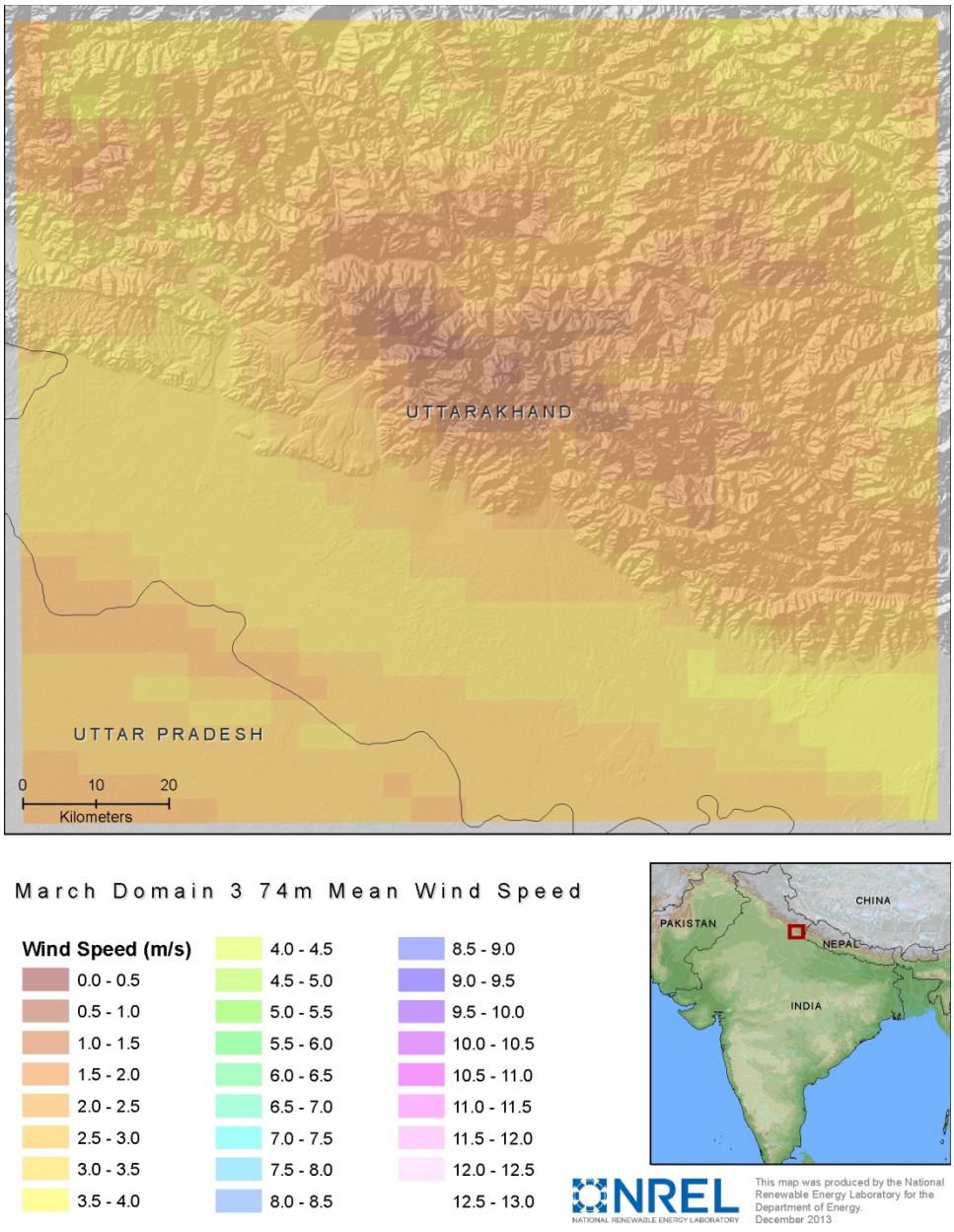

Figure 17: Average wind speed at approximately 80-m above the surface from 3.3-km resolution simulations of 1-8 Mar 2012

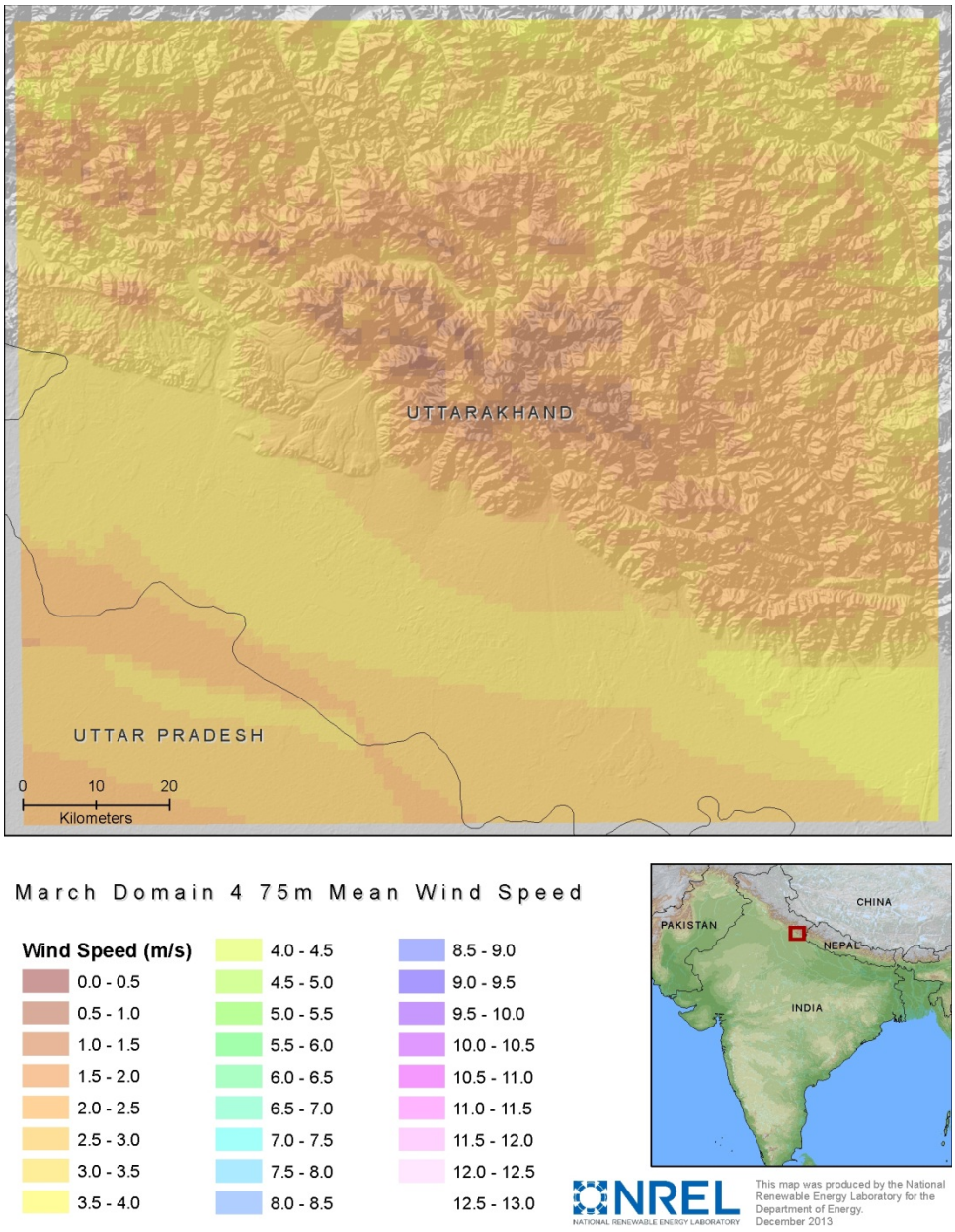

Figure 18: Average wind speed at approximately 80-m above the surface from 1.1-km resolution simulations of 1-8 Mar 2012

3.2 Variability of the Wind Resource with Height

Although current utility-scale turbines have average hub heights on the order of 80 m, new developments in technology are expected to increase hub heights to at least 100 m or more. Wind speeds were extracted from these simulations at approximately 100 m above the surface to explore whether or not more wind resource was available at higher altitudes due to nocturnal jet phenomena (Banta et al., 2002). There was no evidence of a significant increase of averaged

wind speed with height in the averaged wind resource plots for the highest resolution simulations of each season (Figure 19-Figure 21).

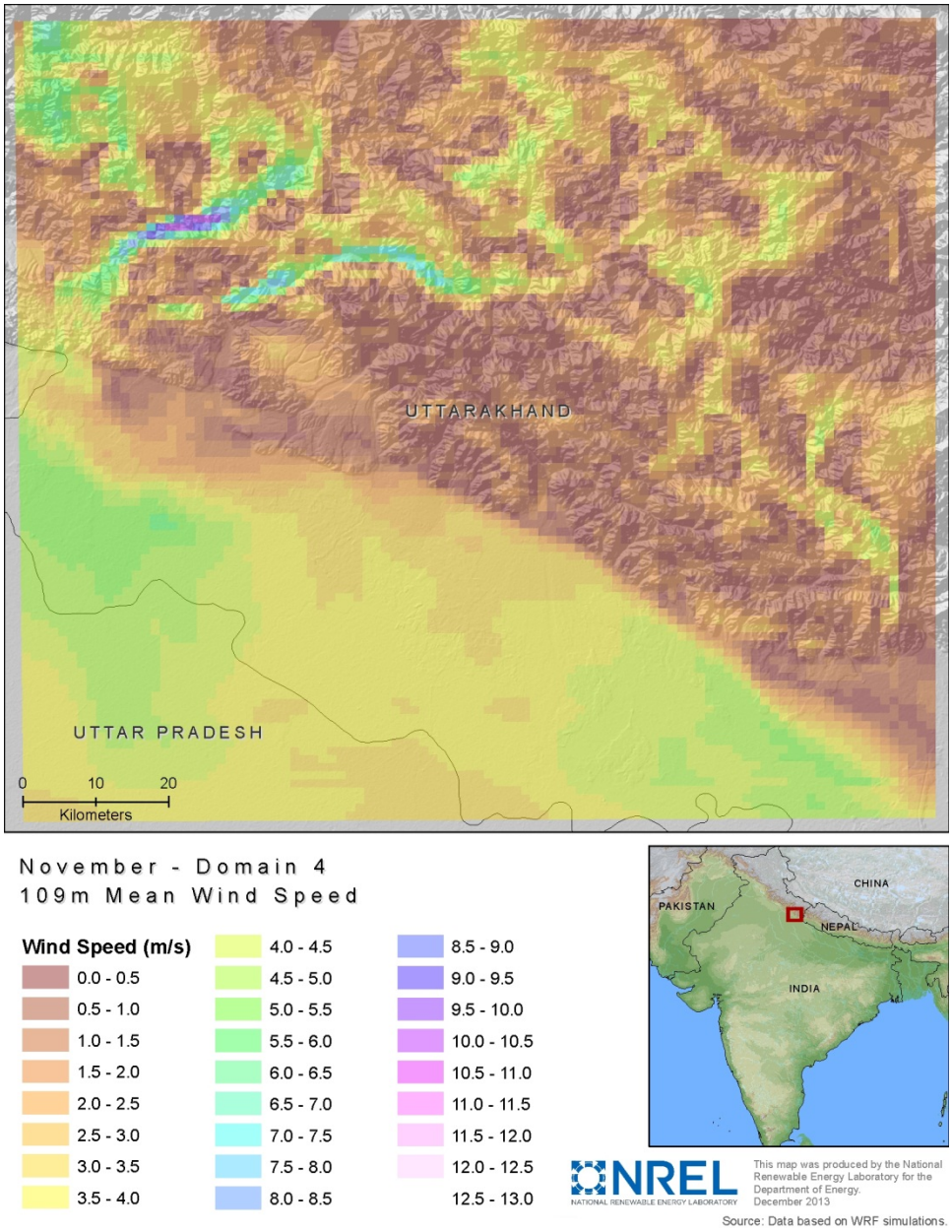

Figure 19: Average wind speed at approximately 100-m above the surface from 1.1-km resolution simulations of 1-7 Nov 2011

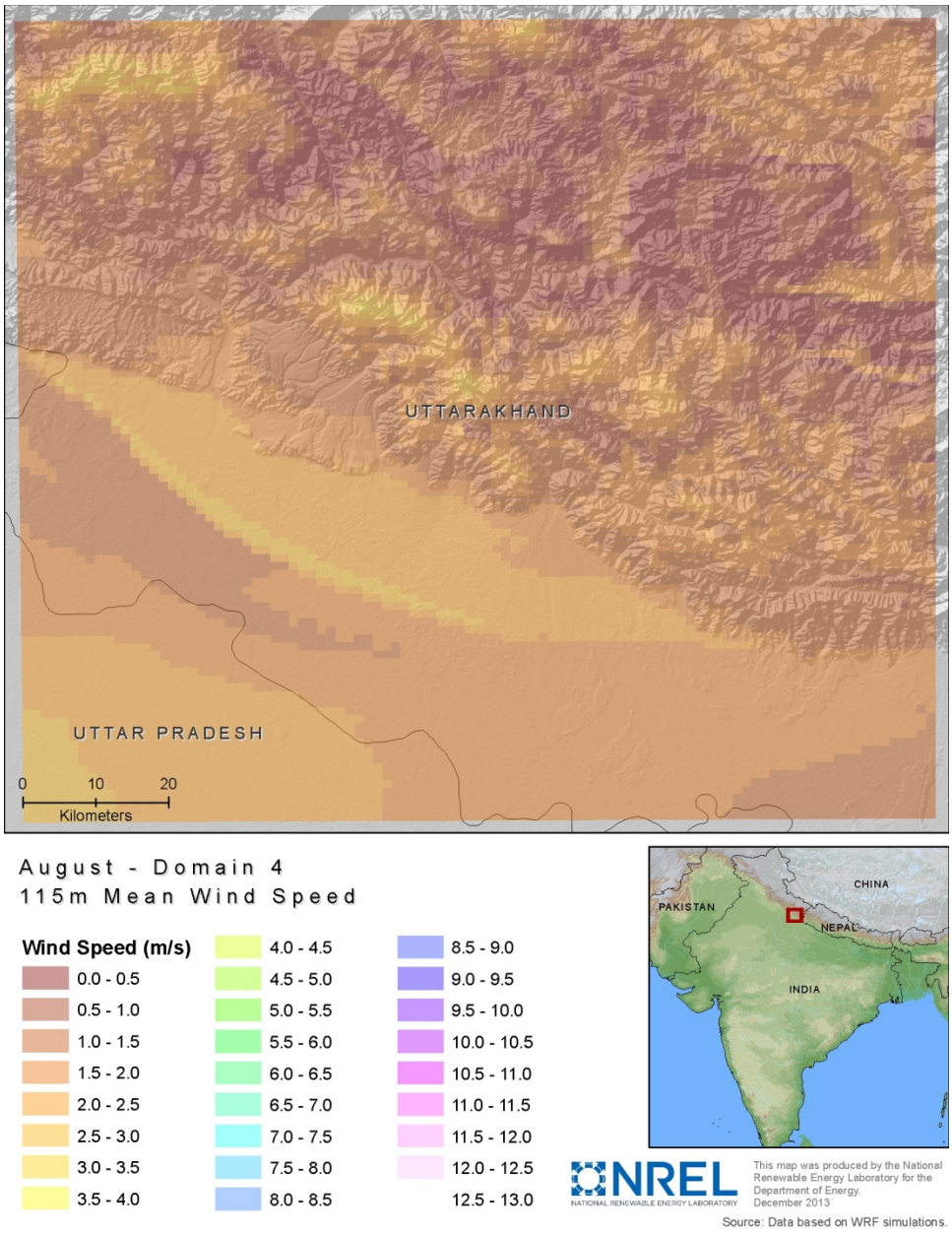

Figure 20: Average wind speed at approximately 100-m above the surface from 1.1-km resolution simulations of 8-15 Aug 2011

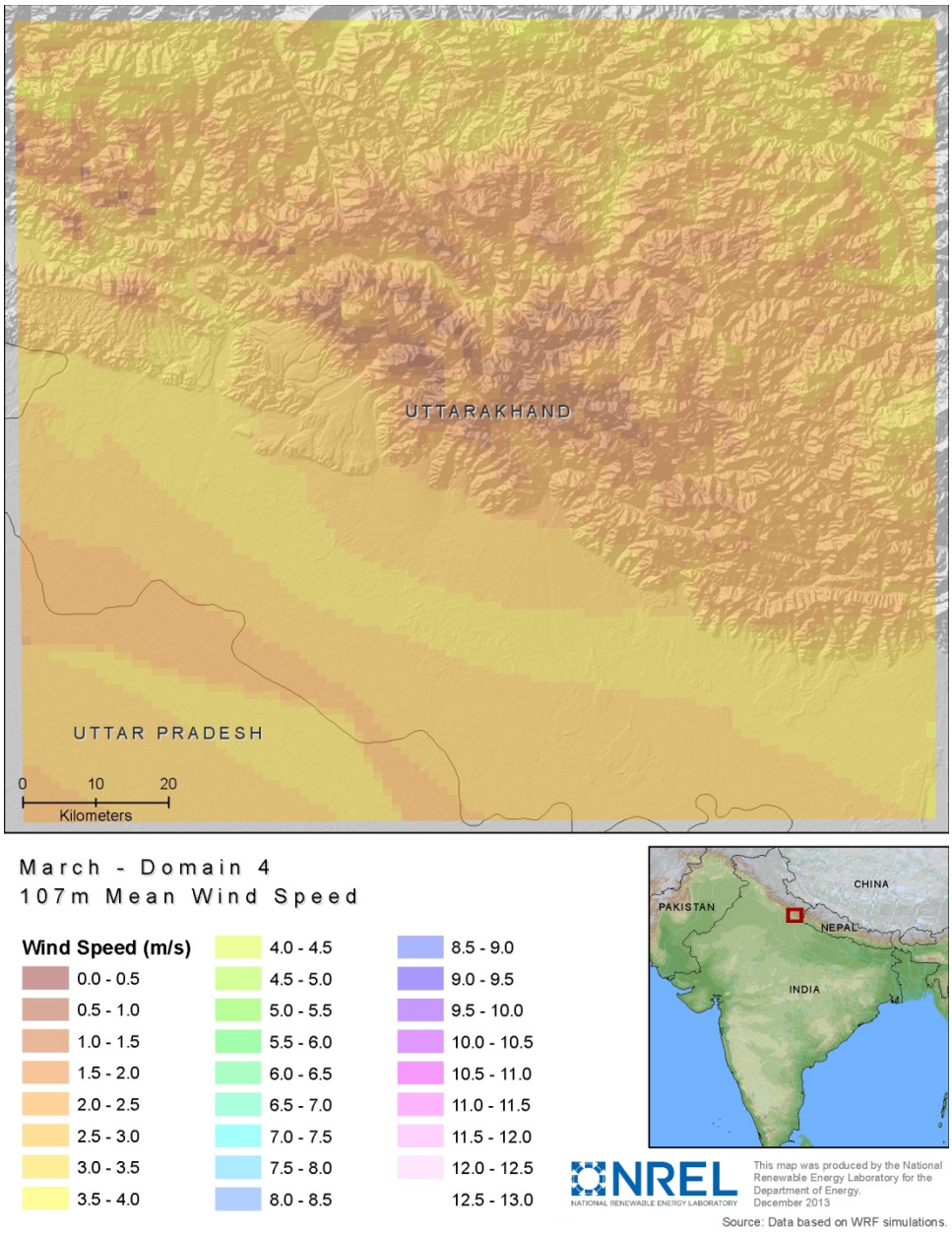

Figure 21: Average wind speed at approximately 100-m above the surface from 1.1-km resolution simulations of 1-8 Mar 2012

3.3 Comparison of Mesoscale Simulations to Lidar Data

Evaluation of simulations, as compared with observations, can rely on several different metrics, typically relying on measurements from multiple locations rather than measurements from one location. Several recent surveys of error and verification metrics for wind energy forecasting (Geibel et al., 2011; Bielecki et al., 2010, among others) have provided useful summaries of performance metrics. Several metrics are commonly presented in assessing wind energy forecasts, yet no individual metric offers a complete description of error tendencies.

Traditionally, mean absolute error (MAE), median absolute error (MDE) and root mean square error (RSME) have been widely used and accepted by the forecasting industry as standard methods for quantification of forecast error. The MAE provides insight about the average magnitude of the errors over an entire dataset; if the forecast error were simply averaged, then positive and negative errors would be cancelled out. Landberg and Watson (1994) emphasize that the use of the mean error would be inaccurate and would lead to misinterpretation as negative and positive errors may be averaged to give a low mean error. However, this advantage of the MAE comes at the expense of losing information about whether the forecast consistently under-predicts or over-predicts wind speeds. This bias can be important. The MDE behaves similarly to the MAE with less sensitivity to outliers. Finally, the Pearson correlation coefficient, R, between observed values and forecast values can indicate general patterns of agreement.

As discussed in detail in the following sections, the general agreement is very poor between the forecasts and the observations at the one available site. Correlation coefficients between a time series of lidar observations and WRF simulations at approximately the same altitude are less than 0.4 between the simulations and the profiles, implying no correlation between the two and underscoring the challenge of numerical weather prediction in such complex terrain. It is surmised that some of the localized terrain forcing in the vicinity of the observation site (within a mountain valley) is not represented in these simulations. Detailed verification of these forecasts would involve multiple observing stations within the simulation domain that preferably measure winds at multiple altitudes (Warner, 2011) and consider other meteorological quantities such as temperature, humidity, and precipitation. A detailed comparison should also involve comparing the wind speed probability distribution functions over a longer period of time. It appears that although the timing is off, the simulations do have some skill in simulating the wind speed variability (e.g., Fig. 23).

3.3.1 Winter

The lidar measurements from the week of November exhibit a moderate average wind speed at hub height of approximately 6.3 m/s. Of the three simulation periods, the November simulations exhibited the highest localized wind speeds, generally constrained to a few valleys in the northwest of the domain. However, the wind resource is generally simulated, on average, as very low, with a mean value in the finest-scale domain of less than 2 m/s (Figure 22). The mean absolute error between the lidar observations and the simulations' predictions at the lidar location greatly exceeds the average wind speed predictions. In the finest domain, the MAE between the WRF simulations and the lidar observations is 4.9 m/s, the MDE is 4.7 m/s, and the RMSE is 5.6 m/s. The WRF simulations clearly failed to capture a mechanism driving the stronger winds observed with the lidar.

3.3.2 Monsoon

The lidar measurements from the selected week in August exhibit a moderate average wind speed at hub height of approximately 6.3 m/s, similar to those of November. However, the WRF simulations suggest much lower average wind speeds in every domain (Figure 23). Only the second domain (10-km horizontal resolution) average wind speed exceeds 3 m/s. In the finest-scale domain, which was expected to be most accurate, the MAE between the WRF simulations and the lidar observations was 3.9 m/s (greater than the average wind speed of 2.9 m/s), the MDE 3.5 m/s, and the RMSE 4.8 m/s, suggesting that the simulations have little skill in

matching the observations at the lidar location. There may be substantial wind resource, as suggested by the observations, but the simulations as designed here cannot represent it.

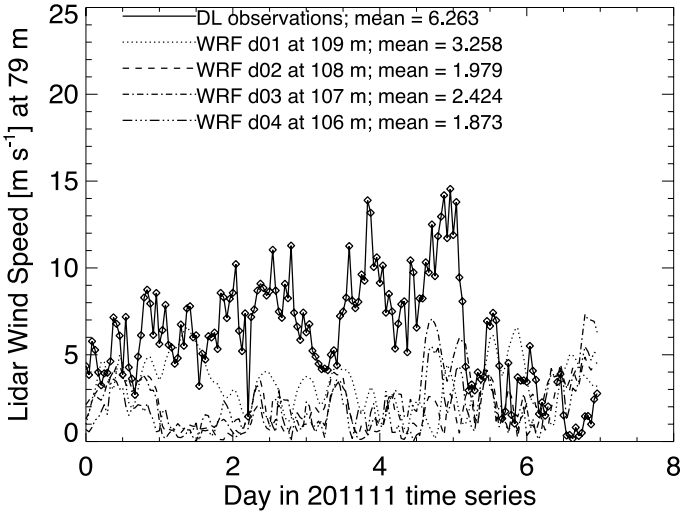

Figure 22: Time series of Doppler lidar winds compared with WRF forecasts from all domains during November simulation period

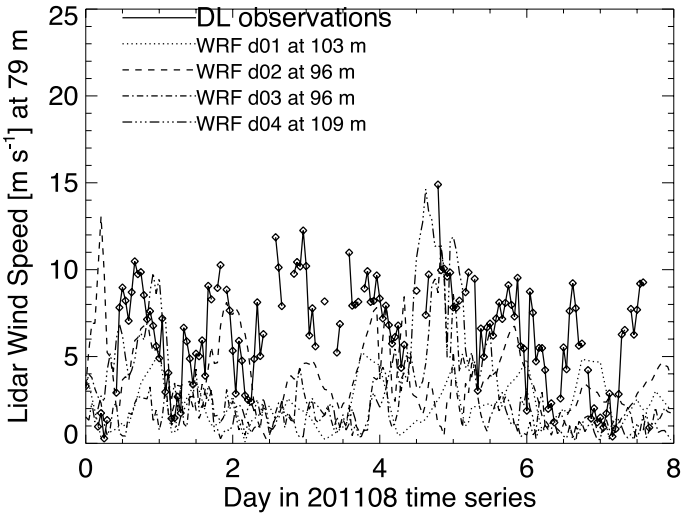

Figure 23: Time series of Doppler lidar winds compared with WRF forecasts from all domains during August simulation period.

3.3.3 Spring

The lidar measurements from the March time period show an average wind speed of 6.7 m/s at hub height, slightly higher than the measurements in November and August. Although the average wind speed in the finest domain of the WRF simulations is also high, 5.2 m/s, there is little agreement between the simulations and the observations, with an MAE of 5.9 m/s, an MDE of 5.9 m/s, and an RMSE of 6.7 m/s. In particular, the distinct shift from a high-wind-speed regime in the first three days of the observations to a lower-wind-speed regime in the last four days of simulations is not represented in the simulations (Figure 24). This wind speed shift, and the physical mechanisms inducing it, could merit closer investigation if a future study seeks to understand the inadequacies of the simulations as executed here.

3.4 Diurnal Variability of the Wind Resource

Even a low average wind resource may be useful if the variation in the wind resource is such that turbines can generate power at times of high demand (Hart et al. 2012). Spectral analysis (not shown) of the lidar observations does not suggest a strong diurnal cycle in any of the seasons analyzed here. Rather, the synoptic signal dominates variability at the location of the lidar observations. A very slight average diurnal signal is seen in the springtime period (Figure 25), with the maximum wind speeds occurring in the evening [13:00 Coordinated Universal Time (UTC) or 18:30 India Standard Time (IST)], late at night (20:00 UTC or 01:30 IST), and early in the morning (1:00 UTC or 6:30 India Standard Time). More observations would be necessary to explore whether the Uttarakhand wind resource variability matches the demand of the New Delhi population center.

3.5 Comparison of Simulations With Existing Wind Resource Assessments for Uttarakhand

The existing wind resource assessment map for Uttarakhand is available from CWET (2013). In aggregate, approximately 534 MW of resource is considered to be available, although measurements are not available to validate that estimate. As the area of Uttarakhand is 53,484 km^2, the CWET estimate assumes a very low wind density of 0.01 MW/km^2. A direct comparison between that estimate and the seasonal simulations executed here is not possible, but the aggregated wind speeds predicted with downscaled WRF are low. The November season simulations here, with the highest values, predict a domain-average wind speed of less than 2 m/s^{-1}. Converting the wind speeds of the entire domain to power, using the power curve of a GE 1.5-MW turbine and assuming a density of one turbine per square kilometer (a relatively coarse spacing of approximately 12.5 rotor diameters between turbines) suggests a density of 0.03 MW/km^2, not accounting for exclusion zones or variability in the wind resource outside of the time period simulated here. Even this rough estimate, based on simulations that likely underestimate the wind resource, is higher than the current estimate of wind resources in Uttarakhand, and suggests that a modest measurement campaign would be warranted to better quantify the possible wind resource.

Of note, the lidar observations suggest wind speeds consistently higher than those predicted by the simulations. Without more observation locations, it is not possible to speculate on the broad availability of the wind resource in Uttarakhand, but **a more extensive wind resource measurement campaign would be justified on the basis of the lidar observations alone**.

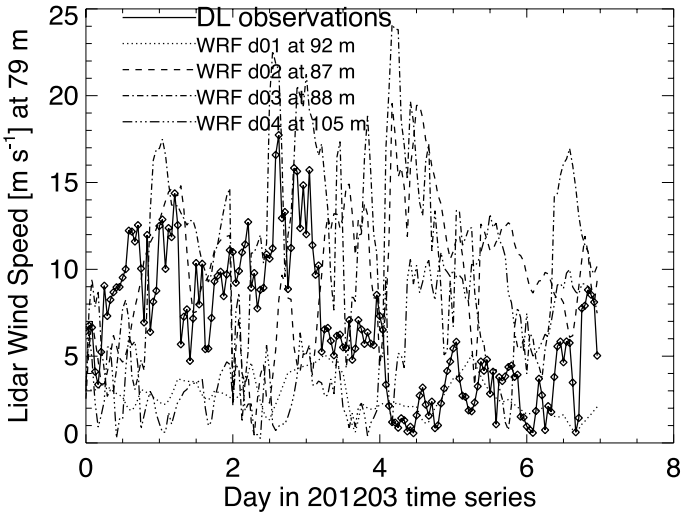

Figure 24: Time series of Doppler lidar winds compared with WRF forecasts from all domains during March simulation period

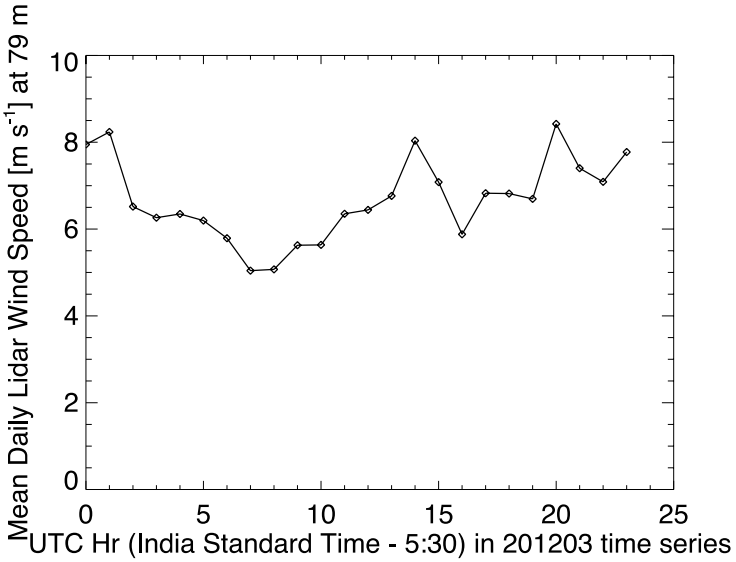

Figure 25: Average diurnal cycle of hub-height winds from lidar observations during the March simulation period

4 Summary and Conclusions

The wind resource in Uttarakhand, India, has been considered to be very low, while the proximity of this region to the large population center of New Delhi implies that modest investments in transmission could enable any wind resources in Uttarakhand to address ongoing energy demands in New Delhi. Very limited observations of the wind resource in Uttarakhand have been carried out, however, a comprehensive wind resource assessment campaign would require observations from multiple locations within the Uttarakhand region. In lieu of a broad measurement campaign, an investigation of possible wind resources in the Uttarakhand region of India has been executed based on dynamically-downscaled simulations with the WRF model. These simulations have been compared with observations from a profiling Doppler lidar deployed by the DOE ARM Program during the Ganges Valley Aerosol Experiment.

Boundary conditions from the Global Forecasting System (1/2 degree in latitude/longitude resolution) were dynamically downscaled with the WRF model at very high resolution in the boundary layer, with thirteen levels in the lowest 300 m to resolve terrain-driven flow. All four domains were centered on the lidar measurement location. Approximately seven days in each of the three different seasons were selected for initial simulations to explore the viability of dynamic downscaling for wind resource assessment in the complex terrain of the Uttarakhand region. These time periods were chosen to sample seasonal variability and for comparison with the GVAX Doppler lidar measurements.

Wind variability over approximately seven days within each of the three different seasons (August 2011, November 2011, and March 2012) has been quantified. The lidar observations during the selected time periods suggest at least modest wind resources, with averages exceeding 6 m/s at nominally 80 m above the surface. The simulations predicted much lower wind speeds: none of the time periods simulated showed evidence of average wind speeds higher than 5 m/s at altitudes nominally 80 m above the surface, indicating that the simulations fail to capture the physical mechanisms giving rise to the winds observed by the lidar. Increasing the horizontal resolution of the simulations and increasing the resolution of the terrain represented in the simulations does not improve the agreement between the simulations and the observations. Traditional model evaluation metrics, such as mean absolute error, median absolute error, and root mean square error, suggest these simulations have poor agreement with the observations. A detailed comparison would involve comparing the wind speed probability distribution functions over a longer period of time. It appears that although the timing is off, the simulations do have some value in simulating the wind speed variability (e.g., Figure 24).

Because the lidar observations indicate that at least one location in Uttarakhand enjoys some wind resources, with a slight diurnal cycle that would provide more power at night, a more extensive measurement campaign in this region could be appropriate. A set of reliable meteorological data sources can be assimilated into future simulations which may incorporate a larger domain and capture the relevant mechanisms driving the flow in Uttarakhand. Recently developed hybrid downscaling techniques, which combine the benefit of statistical and dynamical approaches, could provide accurate multi-year wind resource assessments and reliable quantification of their uncertainty at locations where observations are available for several months and the deterministic numerical weather prediction model is run over the multi-year period.

Acknowledgements

The authors gratefully acknowledge the data visualization efforts of Jennifer Melius and Donna Heimiller of National Renewable Energy Laboratory's (NREL's) Data Analysis and Visualization Group in the Strategic Energy Analysis Center. The WRF simulations were completed using NREL's high-performance computing (HPC) system Redmesa for March 2012 runs, while using NREL's Petascale HPC system Peregrine for August and October/November 2011 runs. The Redmesa used capabilities of the NREL's Computational Science Center, which is supported by the U.S. Department of Energy (DOE) under Contract No. DE-AC36-08GO28308. The research performed on the Peregrine system was done using computational resources sponsored by DOE at NREL. This research was supported by the Office of Biological and Environmental Research of the U.S. Department of Energy as part of the Atmospheric Radiation Measurement Climate Research Facility.

This work was funded by DOE and the U.S. Department of State, under the U.S.-India Energy Dialogue's New Technology and Renewable Energy Working Group. The authors would also like to acknowledge Michael Mills and Elena Berger of DOE for supporting this research and express appreciation to Dr. Luca Delle Monache and Dr. Andrew Monaghan of the National Center for Atmospheric Research for their review of this report.

References

Banta R.M.; Newsom, R.K.; Lundquist, J.K.; Pichugina, Y.L.; Coulter, R.L.; and Mahrt, L.D. (2002) "Nocturnal Low-Level Jet Characteristics Over Kansas during CASES-99," *Boundary-Layer Meteorology* **105**, 221–252.

Browning, K. and Wexler, R. (1968) "The Determination of Kinematic Properties of a Wind Field using Doppler Radar," *Journal of Applied Meteorology* **7**, 105–113.

Brower, M. C., (2012) *Wind Resource Assessment: A Practical Guide to Developing a Wind Project*. Wiley, 296 pages.

Castro, C. L., Pielke Sr., R. A. and Leoncini, G. (2005). Dynamical downscaling: Assessment of value retained and added using the Regional Atmospheric Modeling System (RAMS). *Journal of Geophysical Research*, **110**, D05108, doi:10.1029/2004JD004721.

Clifton, A.; Daniels, M. H.; and Lehning, M. (2013) "Effect of Winds in a Mountain Pass on Turbine Performance." *Wind Energy*. doi: 10.1002/we.1650.

CWET. (2013). Estimation of Installable Wind Power Potential in India at 80 m. http://www.cwet.tn.nic.in/html/departments_ewpp.html Accessed 17 Dec 2013.

Delle Monache**,** L.**;** Eckel, T.; Rife, D.; and Nagarajan, B. (2013) "Probabilistic Weather Prediction with an Analog Ensemble," *Monthly Weather Review*, **141**, 3498-3516.

Dimri, A.; Yasunari, P.T.; Wiltshire, A.; Kumar, P.; Mathison, C.; Ridley, J.; Jacob, D. 2014 "Application of Regional Climate Models to the Indian Winter Monsoon Over the Western Himalayas, *Science of The Total Environment*, Available online 11 February 2013, ISSN 0048-9697. http://dx.doi.org/10.1016/j.scitotenv.2013.01.040. (http://www.sciencedirect.com/science/article/pii/S0048969713000594)

DuVivier, A. K. and Cassano, J. J. (2013) "Evaluation of WRF Model Resolution on Simulated Mesoscale Winds and Surface Fluxes near Greenland." *Monthly Weather Review*, **141**, 941–963. doi: http://dx.doi.org/10.1175/MWR-D-12-00091.1

Giebel, G. (2001) *On the Benefits of Distributed Generation of Wind Energy in Europe*. PhD thesis from the Carl von Ossietzky Universität Oldenburg. Fortschr.-Ber. VDI Reihe 6 Nr. 444. Düsseldorf, VDI Verlag 2001. ISBN 3-18-344406-2.

Hart, E. K., Stoutenburg, E. D.; Jacobson, M. Z. (2012) "The Potential of Intermittent Renewables to Meet Electric Power Demand: Current Methods and Emerging Analytical Techniques." Proceedings of the IEEE, **100**, 322-344. doi:10.1109/JPROC.2011.2144951.

Hossain, J.; Sinha, V.; Kishore, V. V. N. (2011) A GIS-Based Assessment of Potential for Wind Farms in India," *Renewable Energy* **36**, 3257-3267.

Hughes, M.; Neiman, P. J.; Sukovich, E.; and Ralph, M. (2012)" Representation of the Sierra Barrier Jet in 11 Years of a High-Resolution Dynamical Reanalysis Downscaling Compared with Long-Term Wind Profiler Observations," *J. Geophys. Res.,* 117, *D18116, doi:*10.1029/2012JD017869.

Landberg, L. and Watson, S.J. (1994) "Short-term Prediction of Local Wind Conditions," *Boundary-Layer Meteorology* **70**, 171.

Mahoney, B.; Parks, K.; Wiener, G.; Liu, Y.; Myers, W.; Sun, J.; Delle Monache, L.; Hopson, T.; Johnson, D.; Haupt, S. (2012) "A Wind Power Forecasting System to Optimize Grid Integration," *IEEE Transactions on Sustainable Energy*, 3, 670-682.

Ministry of New and Renewable Energy (2013). http://www.mnre.gov.in/mission-and-vision-2/achievements/ Retrieved on 17 Dec 2013.

Nakanishi, M. and Niino, H. (2006) "An Improved Mellor-Yamada Level-3 Model: Its Numerical Stability and Application to a Regional Prediction of Advection Fog." *Boundary-Layer Meteorology*, 119, 39-407.

Newsom, R., (2012). *The DL Handbook*. Available at http://www.arm.gov/publications/tech_reports/handbooks/dl_handbook.pdf , DOE/SC-ARM-TR-101.

Rife, D.L.; Vanvyve, E; Pinto, J.O.; Monaghan, A.J.; Davis, C.A.; Poulos, G.S. (2013) "Selecting Representative Days for More Efficient Dynamical Climate Downscaling: Application to Wind Energy." *J. Appl. Meteor. Climatol.*, **52**, 47–63. doi: http://dx.doi.org/10.1175/JAMC-D-12-016.1

Skamarock, W. C., et al. (2008) "A Description of the Advanced Research WRF Version 3." NCAR Tech. Note NCAR/TN-475+STR, Mesoscale and Microscale Meteorology Division, NCAR, 125 pp. Available online at http://www.mmm.ucar.edu/wrf/users/docs/arw_v3.pdf.

Unidata/University Corporation for Atmospheric Research, National Centers for Environmental Prediction/National Weather Service/NOAA/U.S. Department of Commerce, and European Centre for Medium-Range Weather Forecasts, 2003: Historical Unidata Internet Data Distribution (IDD) Gridded Model Data, December 2002 - current. Research Data Archive at the National Center for Atmospheric Research, Computational and Information Systems Laboratory, Boulder, CO. [Available online at http://rda.ucar.edu/datasets/ds335.0.] Accessed§ 01 Oct 2013.

Warner, T. T. (2011). *Numerical Weather and Climate Prediction.* Cambridge University Press, 548 pp.

Whiteman, D. (2000). *Mountain Meteorology: Fundamentals and Applications*. Oxford University Press. 355 pp.